energies

MDPI

Article

Dependence of the Microporosity of Activated Carbons on the Lignocellulosic Composition of the Precursors

Silvia Román [1,*], Beatriz Ledesma [1], Andrés Álvarez-Murillo [1], Awf Al-Kassir [2] and Talal Yusaf [3]

1 Department of Applied Physics, University of Extremadura (UEX), Avda. Elvas s/n, 06071 Badajoz, Spain; beatrizlc@unex.es (B.L.); andalvarez@unex.es (A.Á.-M.)
2 Department of Mechanical, Energetic and Materials Engineering, University of Extremadura (UEX), Avda. Elvas s/n, 06071 Badajoz, Spain; aawf@unex.es
3 National Centre for Engineering in Agriculture, University of Southern Queensland (UQ), Brisbane, QLD 4350, Australia; talal.yusaf@usq.edu.au
* Correspondence: sroman@unex.es

Academic Editor: Paul L. Chen
Received: 12 January 2017; Accepted: 14 April 2017; Published: 15 April 2017

Abstract: A series of activated carbons were prepared by physical steam gasification under identical experimental conditions to compare the pore development from almond tree pruning chars and walnut shell activated carbons. The results obtained showed that steam gasification yields microporous carbons in both cases, and the rise in temperature causes an increase of the pore volumes of the activated carbons, up to a certain degree of burn-off. This effect was more marked for walnut shell, which gave rise to activated carbons with apparent surface values of up to 1434 $m^2 \cdot g^{-1}$. Also, a slight widening of porosity was found at low burn-off degrees. This pore widening was more marked in the case of activated carbons from almond tree pruning, which also have a high macropore volume. It was found that the lignocellulosic and porosity properties of the raw materials can cause this different behavior towards activation processes.

Keywords: activated carbon; biomass; lignocellulosic composition

1. Introduction

Increasing concerns regarding drinking water contamination and a trend shift towards healthier lifestyles, coupled with increasingly stringing government regulations has increased activated carbon (AC) demand in last years. Recent estimates report the AC market is expected to reach a value of $4.46 billion by 2020, with an annual growth rate of 10.8% [1]. Moreover, both rapid industrialization and increasing government focus on environmental protection are expected to fuel industry growth after 2020, at an even faster rate. In this framework, research on new effective raw materials (different from coconut shell, which still remains as the most used granular AC precursor) is a worldwide research hotspot.

It is well known that the microporous nature of ACs depends on both the precursor and the carbonization and activation conditions. The literature offers abundant examples of research focused on the effect of different variables (temperature, time, addition of chemicals...) on the properties of ACs prepared from a given raw material. However, the study of the influence of the precursor features on the textural and surface characteristics of the resulting ACs is very interesting and has been scantly studied. Among the few pieces of research devoted to this objective, the following ones can be cited: Arriagada et al. [2] related a higher contribution in external area to a higher lignin content. Marsh and Rodríguez-Reinoso [3] associated several physical properties of the raw material (such as hardness

and density) to the porosity of the derived ACs; among these materials, they associated the cellular structure of wood to soft macroporous activated carbons, while they attributed a microporous nature to ACs obtained from fruit shells. In the same line, Chatterjee and Saito [4] have recently provided an interesting review on lignin-derived carbon materials, in which they discuss the influence of lignin proportions on the microstructural properties of carbon materials. These authors state that since lignin is the least reactive substance as compared to cellulose and hemicellulose, it might control the solid yield of the thermal process, which definitely influences the final porosity development; in particular, they associated a greater lignin proportion to a more microporous nature, and a more heterogeneous pore size distribution to cellulose. Dissimilarly, Rodríguez-Correa et al. [5] investigated the influence of lignocellulosic composition and the thermal steps of the pyrolysis process and its subsequent influence on the porosity of KOH activated carbons and found that the presence of cellulose contributed to micropore formation. Furthermore, the work made by Cagnon et al. was very illustrative; these authors performed a study on the thermal behavior of various biomass materials (pure: hemicellulose, cellulose and lignin; and real heterogeneous biomass materials: coconut shell, apple pulp, plum stones, olive stones and a soft wood) upon pyrolysis. They identified differences in thermal events and in reactivity and they developed a predictive model using the results from pure materials, which was also validated for heterogeneous biomass. Furthermore, these authors, steam activated the samples (800 °C) and studied their porosity; they concluded that although a particular pore size distribution (PSD) of isolated materials might make sense (and they related hemicellulose to broader PSD in relation to cellulose and lignin), extrapolating this tendency to heterogeneous biomass was not as straightforward, owing to the chemical interactions between components. In this way, they suggested that lignin was the main contributor to char and AC formation, and that the porosity of the materials was in fact related to the reacted amount of each pure component, which in turn depended of its weight contribution [6].

On the other hand, beyond the lignocellulosic composition, Heschel and Klose [7] found a relation between the porosity of the parent material and the macroporosity of the chars and ACs obtained from various lignocellulosic residues. Excluding the cited work, to the author´s known, this effect has not been studied again.

There is therefore a lack of knowledge and a need to further investigate how the chemical and physical features of raw materials can affect their subsequent activation. With these premises, we studied here the use of two biomass residues extensively generated in Spain: almond tree prunings (ATP) and walnut shells (WS). Both have different fractions of hemicellulose, cellulose and lignin, which might influence their behavior towards a given activation process, thus affecting the porous structure of the derived ACs. From and industrial perspective, it might be very interesting because it would allow to select the appropriate precursor in order to obtain a target material, by application of unique processing conditions. The ACs were prepared by steam physical activation processes, studying the influence of temperature. Steam was chosen as activating agent since it is widely accepted to yield ACs with high pore volumes [2].

2. Materials and Methods

2.1. Raw Materials

The precursors, provided by local manufacturers, were crushed and sieved (1–2 mm). Table 1 shows the lignocellulosic composition of the precursors used as determined according to the Van Soest method [8].

Table 1. Lignocellulosic composition of walnut shell and almond tree pruning.

Source	Component		
	Hemicellulose (%)	**Cellulose (%)**	**Lignin (%)**
Walnut shell (WS)	20.7	40.1	18.2
Almond tree prunning (ATP)	20.1	33.7	25.0

The raw materials were also characterized by mercury porosimetry (AUTOPORE 4900 IV, Micromeritics, Norcross, GA, USA) determining their mesopore and macropore volumes (V_{meP}, V_{maP}) and the mercury density (ρ_{Hg}). Also, the helium density (ρ_{Hg}) was determined by helium stereopicnometry (Quantachrome, Boynton Beach, FL, USA), and the value of porosity (%) was calculated from both densities according to the expression proposed by Heschel and Klose [7].

2.2. Experimental Set-Up

The experimental installation and procedure used have been described in detail elsewhere [9]. Steam activation processes were carried out during 60 min studying the influence of temperature in the range 650–900 °C, using a steam flow rate of 0.2 g·min^{-1}. These experimental conditions were selected in order to favor the production of microporous activated carbons. According to the bibliography, using high temperatures maximize microporosity [10]; on the other hand, the steam flow rate was selected according to previous works which indicated that 0.2 g·min^{-1} is optimal to develop narrow micropores [11].

2.3. Textural Characterization

The textural properties of the chars and ACs were obtained with the aid of N_2 adsorption at 77 K using a semi-automatic adsorption unit (AUTOSORB-1, Quantachrome, Boynton Beach, FL, USA). By suitable models, the N_2 adsorption isotherms were used to calculate: (1) the value of the BET specific surface (S_{BET}), (2) the external surface (S_{EX}) by α_s-method using the reference non-porous solid proposed by Rodríguez-Reinoso et al. [12], and (3) the volume of micropores (V_{mi}) through the Dubinin-Radushkevich equation.

In the case of the chars, due to the known activated diffusion effects associated with N_2 adsorption at 77 K, CO_2 adsorption isotherms at 298 K were also plotted, using a manual volumetric system.

The mesopore (V_{meP}) and macropore (V_{maP}) volumes, mercury density (ρ_{Hg}), helium density (ρ_{Hg}) and total pore volume (V_t) were also determined for the chars and ACs, as previously described for the raw materials.

The surface morphology of some selected samples was examined by Scanning electron microscopy (SEM; Tokio, Japan,). SEM samples were prepared by depositing about 50 mg of the char on an aluminum stud covered with conductive adhesive carbon tapes, and then coating with Rh–Pd for 1 min to prevent charging during observations. Imaging was done in the high vacuum mode at an accelerating voltage of 20 kV, using secondary electrons.

3. Results and Discussion

3.1. Textural Characterization of Raw Materials and Chars

The pyrolysis process showed a solid yield of 26.8 and 24.0%, for ATP and WS, respectively. These results are in agreement with previous works, which relate higher lignin contents to higher solid yields in carbonization process under these conditions [13].

Figure 1 shows the mercury intrusion curves of the raw materials (AT-Pruning and W-Shell) and chars (C-AT-Pruning and C-W-Shell). Table 2 shows the values of ρ_{Hg}, ρ_{He} and porosity (%) determined from them and the relation V_{maP}/V_{meP} from the intrusion data.

Table 2. Textural characteristics of natural materials and chars.

Material	ρ_{Hg} (g·cm^{-3})	ρ_{He} (g·cm^{-3})	Porosity (%)	V_{maP}/V_{meP}
AT-Pruning	0.712	1.486	52.04	7.944
W-Shell	1.027	1.501	31.59	2.564
C-AT-Pruning	0.378	1.631	76.82	10.140
C-W-Shell	0.665	1.523	56.34	2.555

Porosity (%) calculated from apparent (ρ_{Hg}) and true density (ρ_{He}) from: $100\cdot(1 - \rho_{Hg}/\rho_{He})$.

As it can be deduced from Table 2, the porosity (%) of the residues seems to influence the one found in the char. On the other hand, from Figure 1 it can be seen that the carbonization process gives rise to a great development of meso and macroporosity. Also, this development maintains to a certain extent the meso-macro distribution of the parent material; which can be observed from both Table 2 (see the ratio V_{meP}/V_{maP}) and Figure 1, where the shape of the curves in the lower pore size region indicates that WS presents a higher volume of narrow mesopores while they are almost negligible in the case of ATP. As it can be observed, this trend is also found after carbonization. The precursor composition might also have an effect on the pore development of the char after pyrolyisis. Previous studies have reported that porosity formation might be favored for materials with a high content on hemicellulose and cellulose, since these are the components degraded upon pyrolyisis. Upon devolatilization, oxygen and hydrogen are removed leaving behind a higher concentration of carbon in the char. Dissimilarly, lignin can be degraded in a wider temperature range, and its more resistant fractions need higher temperatures to be fully decomposed (up to 850 °C) [14,15].

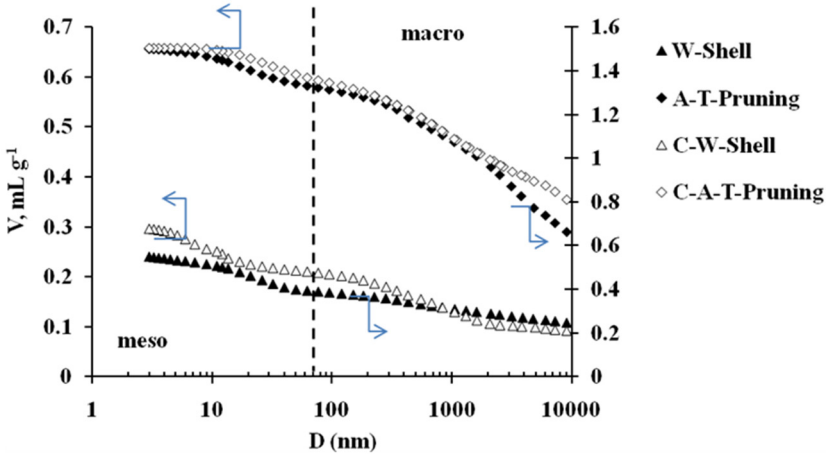

Figure 1. Mercury intrusion curves of chars and raw materials.

The chars were also characterized with respect to their N_2 and CO_2 adsorption at 77 K and 273 K, respectively. From N_2 adsorption data, the values of S_{BET} and V_{mi} were determined; from CO_2 adsorption, W_0 was calculated. These parameters are shown in Table 3.

Table 3. Textural parameters as determined from adsorption of N_2 at 77 K and CO_2 at 273 K.

Char	S_{BET}	V_{mi}	W_0
	$m^2 \cdot g^{-1}$	$cm^3 \cdot g^{-1}$	$cm^3 \cdot g^{-1}$
C-WS	280	0.138	0.458
C-ATP	204	0.097	0.426

As it can be seen, both chars have moderate S_{BET} values, as usually found for lignocellulosic materials; although this porosity should be referred to as "incipient porosity", its lower or greater development is influenced by the different stages associated to thermal degradation which, in turn, depends on its proportion of cellulose, hemicellulose and lignin [16]. On the other hand, in both cases the micropore volume determined by N_2 adsorption is higher than that corresponding to CO_2 adsorption. This fact is usually found in chars, in which the porosity is partially blocked as a consequence of the condensation of products evolved during pyrolysis, and therefore the N_2 at 77 K is not totally diffused to the inner of the particle. The restricted accessibility of N_2 a 77 K seems to be less for C-ATP, as deduced from the lower difference between V_{mi} and W_0, indicating a less constricted or wider pore size material.

3.2. Preparation of Activated Carbons

Figure 2 shows the evolution of the AC burn-off degree upon activation with temperature. As it can be observed, the effect of this variable is more marked for ATP series, indicating a higher reactivity of this precursor towards steam activation processes. This result might be unexpected, since precursors with a higher lignin content have previously been related to lower reactivity; however, at this point it is important to highlight that lignin from different sources show a very dissimilar behavior from each other [4]. In this way, these results might suggest that lignin from AS is less reactive than that of ATP.

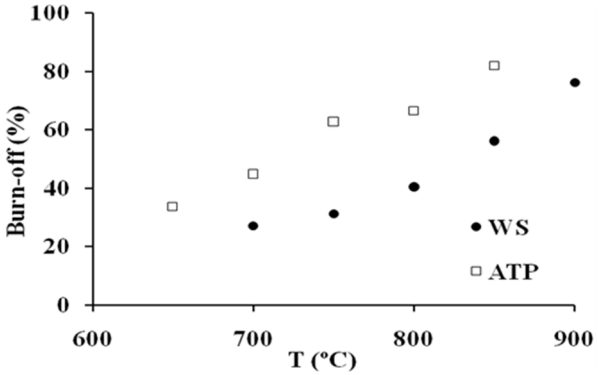

Figure 2. Evolution of burn-off degree with temperature.

3.3. Textural Characterization of Activated Carbons

The AC N_2 adsorption isotherms (a) and corresponding α-plots (b) are shown in Figures 3 and 4, respectively. In these Figures, the ACs have been denoted according to the following nomenclature PR/ST/b, where PR represents the precursor, S means steam, used as activating agent in both series, T stands for activation temperature, and b means the burn-off degree attained in each case. Typical parameters determined from N_2 adsorption data are collected in Table 4.

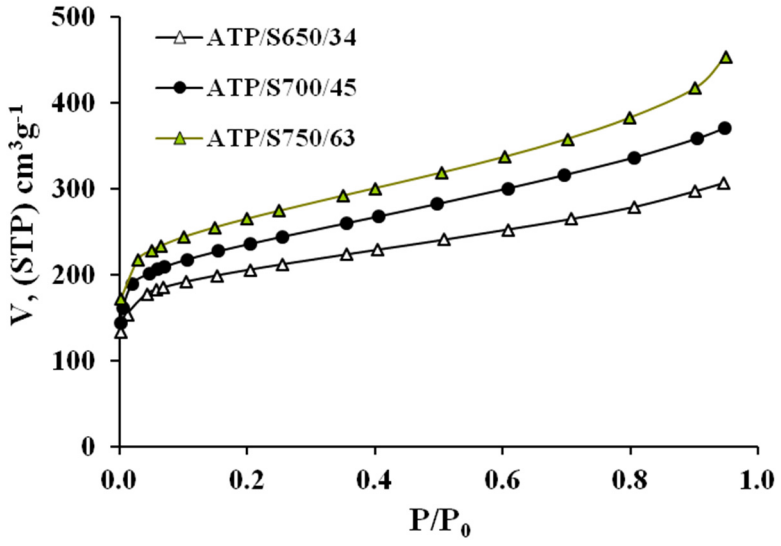

(**a**)

Figure 3. *Cont.*

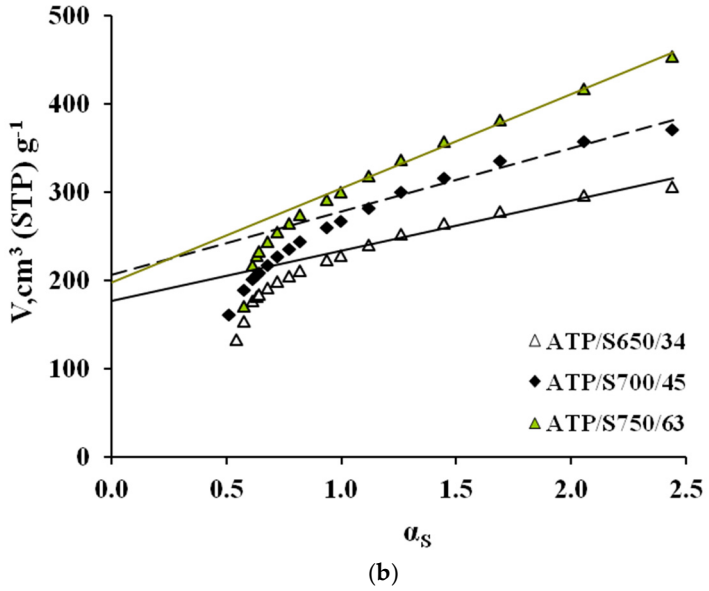

Figure 3. (**a**) N_2 adsorption isotherms at 77 K and (**b**) corresponding alfa plots of ACs prepared from ATP.

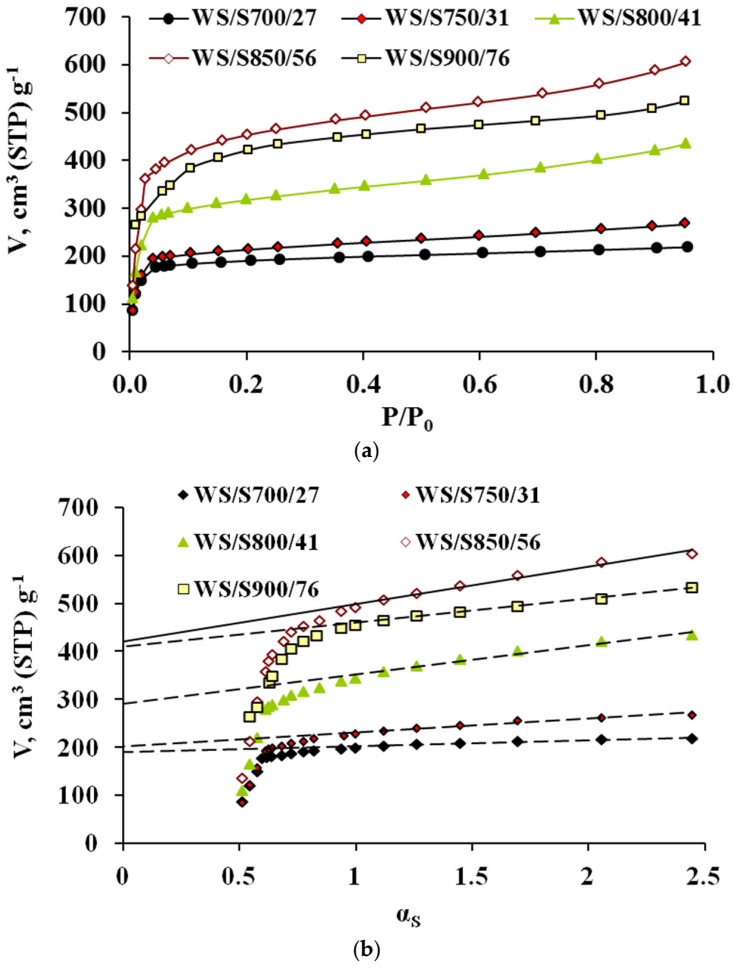

Figure 4. (**a**) N_2 adsorption isotherms at 77 K and (**b**) corresponding alfa plots of ACs prepared from WS.

Table 4. Textural characteristics determined from N_2 adsorption isotherms at 77 K.

Adsorbent	S_{BET}	V_{mi}	V_{me}	S_{EXT}	S_{INT}
	($m^2 \cdot g^{-1}$)	($cm^3 \cdot g^{-1}$)	($cm^3 \cdot g^{-1}$)	($m^2 \cdot g^{-1}$)	(%)
ATP/S650/34	651	0.34	0.14	137	79
ATP/S700/45	755	0.38	0.19	205	73
ATP/S750/63	857	0.43	0.27	268	69
WS/S700/27	573	0.30	0.04	39	93
WS/S750/31	656	0.32	0.10	69	90
WS/S800/41	994	0.52	0.15	158	84
WS/S850/56	1434	0.74	0.20	203	86
WS/S900/76	1339	0.72	0.09	165	88

From Figures 3 and 4 it can be seen that all isotherms are of type I [17], typical of microporous materials. However, a difference can be highlighted from the shape of the isotherms of the different precursors; while the isotherms of WS series have a low slope in the multilayer region (and thus, a low contribution of mesoporosity), the ATP curves show a continuous increase along all the relative pressure interval, which indicates a wider microporosity and a higher contribution of external area. This effect gets more evident for greater burn-off values. Moreover, the greater reactivity shown by ATP upon pyrolysis is found again for activation processes. In all cases, similar activation conditions yield a greater burn-off degree for this material, which definitely will influence the porosity development, as shown below.

Also, the N_2 adsorption capacity is enhanced for higher temperatures, up to certain burn-off value (82 and 76% for ATP and WS series, respectively), at which the external burning of the carbon might be eventually taking place, as it has been previously found during steam activation [3]. As seen in Table 4, increasing temperature from 650 to 700 for ATP series, causes a decrease in the $\%S_{INT}$ contribution from 79 to 73%. In the case of WS, rising the temperature from 700 to 800 °C varies the $\%S_{INT}$ from 93 to 84%. In previous works, it has been found that during steam activation the creation of microporosity is mainly favoured at low burn-off degrees, and that as burn-off is increased, there is a widening of micropores [3]. In these works, the cutting point between the creation and widening of microporosity was found at around 40% and, above this value, the amount of microporosity that was being created was less than that becoming mesoporosity or macroporosity. The results obtained here are in agreement with this hypothesis.

These facts can be also derived from the AC textural characteristics (Table 5). It can also be observed that the values of S_{BET} are similar to those obtained by other authors under similar activation conditions, using other lignocellulosic materials [18].

Table 5. Textural characteristics determined from Hg porosimetry and He stereopicnometry.

	V_{meP}	V_{maP}	ρ_{Hg}	ρ_{He}	V_t
	($cm^3 \cdot g^{-1}$)	($cm^3 \cdot g^{-1}$)	($g \cdot cm^3$)	($g \cdot cm^3$)	($cm^3 \cdot g^{-1}$)
ATP/S650/34	0.30	2.00	0.32	1.93	3.64
ATP/S700/45	0.33	2.15	0.31	1.98	3.78
ATP/S750/63	0.32	2.64	0.26	2.21	4.34
WS/S700/27	0.20	1.22	0.43	2.17	1.86
WS/S750/31	0.21	1.23	0.43	2.15	1.84
WS/S800/41	0.21	0.67	0.56	1.99	1.27
WS/S850/56	0.23	0.64	0.57	2.01	1.25
WS/S900/76	0.30	1.32	0.39	2.12	2.13

It has to be highlighted that the effect of temperature on the porosity development is much more marked in the case of AS series. For this precursor, ACs with high values of V_{mi} (up to 0.74 $cm^3 \cdot g^{-1}$) were obtained for a burn-off degree of 56%. Also, ATP ACs presented lower values of V_{mi}, reaching a maximum of 0.43 $cm^3 \cdot g^{-1}$ for a burn-off degree of 63%, although the external surface contribution was outstanding for this raw material. From these results, it could be concluded that the best precursor if a microporous structured is aimed would be WS. ATP would be preferable just in the

case that the targeted structure was mesoporous. At first glance, this might suggest that lower lignin content is more prone to develop wider pores [4]. Dissimilarly, this hypothesis is in disagreement with other works which stated that cellulose lead to enhanced microporosity development as compared lignin [5].

This controversy suggests that relating lignin proportion to AC porous structure is not as straightforward. Carrot et al. [19] studied lignin-based ACs produced by physical activation and found that lignin from different sources generated porous solids with different textural properties. From our results it is evident that the lignin present in ATP is more reactive and this corresponds not only to larger pores but also to an enhanced widening effect as temperature is increased. A plausible explanation for this effect could rely on the different reactivity of the chars towards steam, under the conditions studied. The main chemical reaction taking place in steam activation process is:

$$C_F + H_2O \rightarrow CO + H_2 \quad (1)$$

where C_F represents a free C atom in the carbon surface, available to participate in the gasification reaction. During gasification, the proper activation within the internal surface does not only depend on the chemical reaction of the gases with the solid surface, but also on the diffusion between the reactive gas (H_2O) and the product gases (CO and H_2) through the porous structure of the carbon and the limit layer surrounding the solid.

Thus, a higher intrinsic reactivity implies that the diffusion of the activating agent (from the limit layer towards the inner of the particle) might not be enough to maintain the reaction on the whole surface (especially on the internal surface). In other words, the higher the reactivity, the greater the steam concentration difference between the internal and external surface, being lower in the internal surface because steam is there mixed with the reaction products. As a consequence, the internal surface area accessible to the gasifying agent is less, and the reaction takes place more easily in the external surface of the particle, as it happens for ATP.

The textural parameters obtained from Hg intrusion and He density analyses, which were made on those ACs presenting the most interesting textural characteristics, are shown in Table 5. The high values of V_{maP} corresponding to ATP series support the greater contribution of gasification on the external surface of the particle, in comparison with WS.

It can be stated that while mesoporosity does not seem to be affected by activation in any case, the values of V_{maP} are clearly increased for ATP series, while they show a variable behavior in WS series. The large V_{maP} values found for ATP series suggest that these ACs might be used for bulky molecules liquid phase applications, while the ACs obtained from WS series could be rather used for gas application or lower size molecules liquid adsorption processes.

The structural features of the porous solids were also studied SEM observation. For the sake of brevity, only the images of two representative samples with similar burn-off degrees (WS/S850/56 and ATP/S750/63) have been collected in Figures 5 and 6.

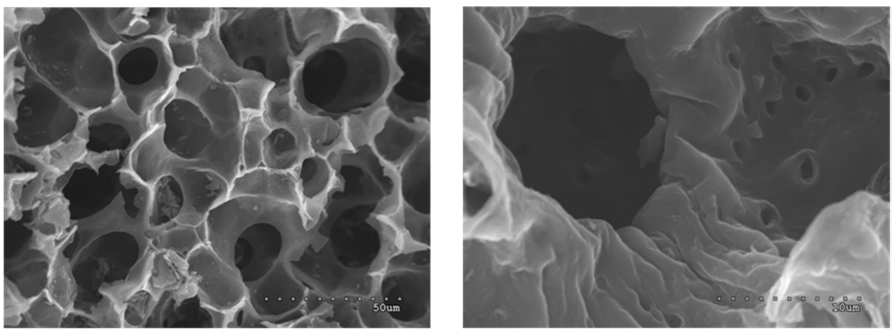

(**a**) (**b**)

Figure 5. SEM micrographs of walnut shell AC (WS/S850/56). Magnification: (**a**) 2000 and (**b**) 10,000.

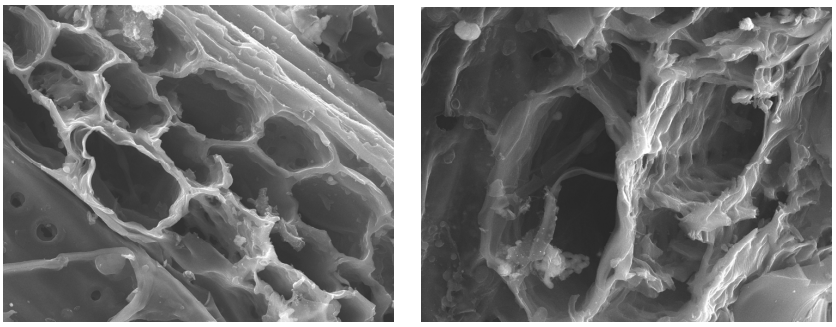

(**a**) (**b**)

Figure 6. SEM micrographs of almond pruning AC (ATP/S750/63). Magnification: (**a**) 1500 and (**b**) 8000.

For both cases, the micrographs of the transverse cross-section of the materials show that the cell structure of each biomass type is still visible after the treatment. Besides, the differences on the porosity of each materials, already inferred from previous analyses, are also deduced from the images. For example, while ATP AC presents beehive-shaped greater cavities, the surface of WS material has cylindrical chimney-like pores. Also, further porosity can be observed at the walls of the pores, and some white small particles can be visualized. These particles, previously reported in previous works, can be associated to the mineral content of the precursor, which undergoes pitting processes as a consequence of the thermal treatment [11].

4. Conclusions

Almond tree prunings and walnut shell are suitable precursors for the preparation of activated carbons with high micropore volumes by physical steam activation processes. Moreover, their pore features can be tuned up by increasing temperature, which causes a rise in the pore volumes in both cases (especially for walnut shell). Moreover, a higher contribution of external area is found for almond tree pruning activated carbons under any temperature condition. The convenience of using walnut shell or almond tree pruning depends on the target porous structure, although at first glance the former would be more interesting because it yields activated carbons with higher apparent area, involving lower burn-off degrees. Improved knowledge on the precursor features influencing final porosity can be really useful and can help control the processes used to yield targeted materials, which can be very significant for increasing the AC market.

Acknowledgments: The authors would like to express their gratitude to the University of Extremadura and the Ministerio de Economía y Competitividad for the financial support received through projects GR15034 and CTM2016-75937-R.

Author Contributions: Silvia Román designed the experiments, reviewed the literatures, and wrote the manuscript; Beatriz Ledesma produced the activated carbons and revised the data; Andrés Álvarez-Murillo contributed to analysis methods; Awf Al-Kassir and Talal Yusaf assisted in the literature review and revised the manuscript.

Conflicts of Interest: The authors declare no conflict of interest.

Nomenclature

S_{BET}	BET specific surface ($J \cdot kg^{-1} \cdot K^{-1}$)
S_{EXT}	External surface ($J \cdot kg^{-1} \cdot K^{-1}$)
S_{INT}	Internal surface proportion (%)
V_{mi}	micropore volume ($cm^3 \cdot g^1$)
V_{me}	mesopore volume ($cm^3 \cdot g^1$)
V_{mep}	mesopore volume, determined by Hg porosimetry ($cm^3 \cdot g^1$)
V_{map}	macropore volume ($cm^3 \cdot g^1$)
V_t	total pore volume ($cm^3 \cdot g^1$)

ρ_{Hg}	mercury density ($g \cdot cm^{-3}$)
ρ_{He}	helium density ($g \cdot cm^{-3}$)

Abbreviations

AC	activated carbon
UEX	University of Extremadura
UQ	University of Queensland
ATP	almond tree pruning
WS	walnut shell

References

1. Global Activated Carbon Trends and Forecasts. Available online: http://www.acarbons.com/global-activated-carbon-market-trends-and-forecasts/ (accessed on 12 January 2017).
2. Arriagada, R.; Garcia, R.; Molina-Sabio, M.; Rodriguez-Reinoso, F. Effect of steam activation on the porosity and chemical nature of activated carbons from eucalyptus-globulus and peach stones. *Microporous Mater.* **1997**, *8*, 123–130. [CrossRef]
3. Marsh, H.; Rodríguez-Reinoso, F. Activation processes (thermal or physical). In *Activated Carbon*, 1st ed.; Elsevier Science: Oxford, UK, 2006.
4. Chatterjee, S.; Saito, T. Lignin-derived advanced carbon materials. *ChemSusChem* **2015**, *8*, 3941–3958. [CrossRef] [PubMed]
5. Correa, C.R.; Otto, T.; Kruse, A. Influence of the biomass components on the pore formation of activated carbon. *Biomass Bioenergy* **2017**, *97*, 53–64. [CrossRef]
6. Cagnon, B.; Py, X.; Guillot, A.; Stoeckli, F.; Chambat, G. Contributions of hemicellulose, cellulose and lignin to the mass and the porous properties of chars and steam activated carbons from various lignocellulosic precursors. *Bioresour. Technol.* **2009**, *100*, 292–298. [CrossRef] [PubMed]
7. Heschel, W.; Klose, E. On the suitability of agricultural by-products for the manufacture of granular activated carbon. *Fuel* **1995**, *74*, 1786–1791. [CrossRef]
8. Roberson, J.B.; Van Soest, P.J. *The Analysis of Dietary Fibre in Food*; James, W.P.T., Theander, O., Eds.; Marcel Dekker: New York, NY, USA, 1981; p. 123.
9. González, J.F.; Encinar, J.M.; González-García, C.M.; Sabio, E.; Ramiro, A.; Canito, J.L.; Gañán, J. Preparation of activated carbons from used tyres by gasification with steam and carbon dioxide. *Appl. Surf. Sci.* **2006**, *252*, 5999–6004. [CrossRef]
10. Giudicianni, P.; Cardone, G.; Ragucci, R. Cellulose, hemicellulose and lignin slow steam pyrolysis: Thermal decomposition of biomass components mixtures. *J. Anal. Appl. Pyrolysis* **2013**, *100*, 213–222. [CrossRef]
11. Román, S.; Ledesma, B.; Álvarez-Murillo, A.; González, J.F. Comparative study on the thermal reactivation of spent adsorbents. *Fuel Process. Technol.* **2013**, *116*, 358–365. [CrossRef]
12. Rodríguez-Reinoso, F.; Martín-Martínez, J.M.; Prado-Burguete, C.; McEnaney, B. A standard adsorption isotherm for the activated carbons. *J. Phys. Chem. A* **1987**, *91*, 515–516. [CrossRef]
13. Zanzi, R.; Sjöström, K.; Björnbom, E. Rapid pyrolysis of agricultural residues at high temperature. *Biomass Bioenergy* **2002**, *23*, 357–366. [CrossRef]
14. Muley, P.D.; Henkel, C.; Abdollahi, K.K.; Marculescu, C.; Boldor, D. A critical comparison of pyrolysis of cellulose, lignin, and pine sawdust using an induction heating reactor. *Energy Convers. Manag.* **2016**, *117*, 273–280. [CrossRef]
15. Coromin, H.M.; Walsh, D.A.; Mokaya, R. Biomass-derived activated carbon with simultaneously enhanced CO_2 uptake for both pre and post combustion capture applications. *J. Mater. Chem. A* **2016**, *4*, 280–289. [CrossRef]
16. Stefanidisa, S.D.; Kalogiannis, K.G.; Iliopouloua, E.F.; Michailofa, C.M.; Pilavachib, P.A.; Lappasa, A.A. A study of lignocellulosic biomass pyrolysis via the pyrolysis of cellulose, hemicellulose and lignin. *J. Anal. Appl. Pyrolysis* **2014**, *105*, 143–150. [CrossRef]
17. Sing, K.S.W.; Everett, D.H.; Haul, R.A.W.; Moscou, L.; Pierotti, R.A.; Siemieinewska, T. Reporting physisorption data for gas/solid systems with special reference to the determination of surface area and porosity (Recommendations 1984). *Pure Appl. Chem.* **1985**, *57*, 603–619. [CrossRef]

18. Selvaraju, G.; Abu Bakar, N.K. Production of a new industrially viable green-activated carbon from Artocarpus integer fruit processing waste and evaluation of its chemical, morphological and adsorption properties. *J. Clean. Prod.* **2017**, *141*, 989–999. [CrossRef]
19. Carrot, P.J.M.; Suhas; Carrott, M.M.L.R.; Guerrero, C.I.; Delgado, L.A. Reactivity and porosity development during pyrolysis and physical activation in CO_2 or steam of kraft and hydrolytic lignins. *J. Anal. Appl. Pyrolysis* **2008**, *82*, 264–271. [CrossRef]